

Diffusion Across Skin

Diffusion of Lidocaine

Shruti Davey

Nirav Patel

BENG 221 – Fall 2011

Introduction

The skin functions as the main physical barrier protecting the body from the external environment. This protective barrier, depicted in Figure 1 [1] is divided into three parts, each with different diffusion coefficients. First on the outside is the stratum corneum, which has the lowest diffusion coefficient of the three. The stratum corneum consists of “keratin-filled, biologically inactive, dried, flattened cells” [1]. This layer, as a whole, is continuous, with very little void space, and “provides almost all of the mechanical strength of the epidermis. The next layer is the epidermis basal layer that provides a steady supply of cells to the stratum corneum to maintain itself [1]. Last is the dermis.

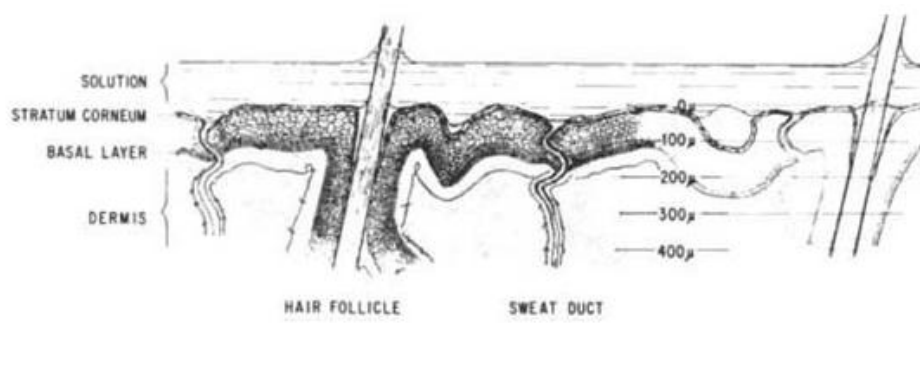


Figure 1 [1]. Depiction of the different layers of human skin. The stratum corneum, basal layer, and the dermis form the three separate layers. This specific image, with the dimension values, focuses on abdominal skin.

Considering the diffusion properties of the layers, it is apparent that the stratum corneum plays the most important role in protecting the internal environment of the body from external factors. Factors that contribute to increases in skin permeability to substances are generally considered to fall into one of the following groups [1]:

- (1) certain substances, such as strong therapeutic drugs and toxins, are capable of diffusing across the skin despite low concentrations present on the surface
- (2) certain substances are capable of affecting the permeability of the skin as they diffuse across.

The focus of this bioengineering problem solving is diffusion of therapeutic drugs across the skin. Therapeutic patches are available for many medical uses, and one such use is a lidocaine patch [2]. One specific example of the benefit of lidocaine therapeutic patch is the pain relief it provides to patients with postherpetic neuralgia [2]. Postherpetic neuralgia, a chronic pain disorder, usually occurs after people have suffered from herpes zoster, commonly known as shingles [3]. Shingles is a result of reactivation of dormant virus that had caused chickenpox in the patients years ago [4]. Nerve damage during shingles is stated as the cause of postherpetic neuralgia [3]. Lidocaine, in this case, serves as a local anesthetic that provides temporary pain relief [2, 3, 5]. One study considered a patch without lidocaine versus a patch with lidocaine on the benefits in pain relief for these patients [2]. The results indicated that the patch with lidocaine definitely provided greater relief. Additionally, the study determined that there was little to no side effects from the use of the lidocaine patch, and that the blood levels of lidocaine were not significant [2]. The therapeutic effects are thought to come from blocking of sodium channels, which in turn decrease “ectopic discharges from damaged peripheral sensory nerves” [2].

Problem Statement

This lidocaine therapeutic patch applies to bioengineering in that the therapy involves diffusion of lidocaine molecules across skin. The diffusion properties is a function of the membrane and the drug molecules, and in this problem solving, a simplified model of diffusion of drug molecules across skin is solved analytically and numerically.

Separation of variables is the mathematical process used in solving the partial differential equation analytically. Several simplifications are made to the realistic model, in order to solve the problem using separation of variables method. The simplifications entail certain assumptions listed below:

- (1) The skin is modeled as a homogeneous slab with surface area that is much greater than the total thickness. This assumes that all three layers of the skin have the same diffusion coefficient, and in effect form one slab. In addition, the intrinsic inhomogeneity of the layers are not considered. Any variations in the thickness, diffusion across sweat ducts, hair follicles, any short pathways, and other surface defects are not considered.
- (2) The therapeutic patch, attached to the skin, is infinitely thin. Therefore, volume is negligible.
- (3) Microcirculation in the capillaries carries the drug molecules away from the site at a very fast rate, maintaining the inner concentration at 0.
- (4) The change in concentration in the patch is minimal, such that assumption of zero flux at the patch-skin interface is valid.

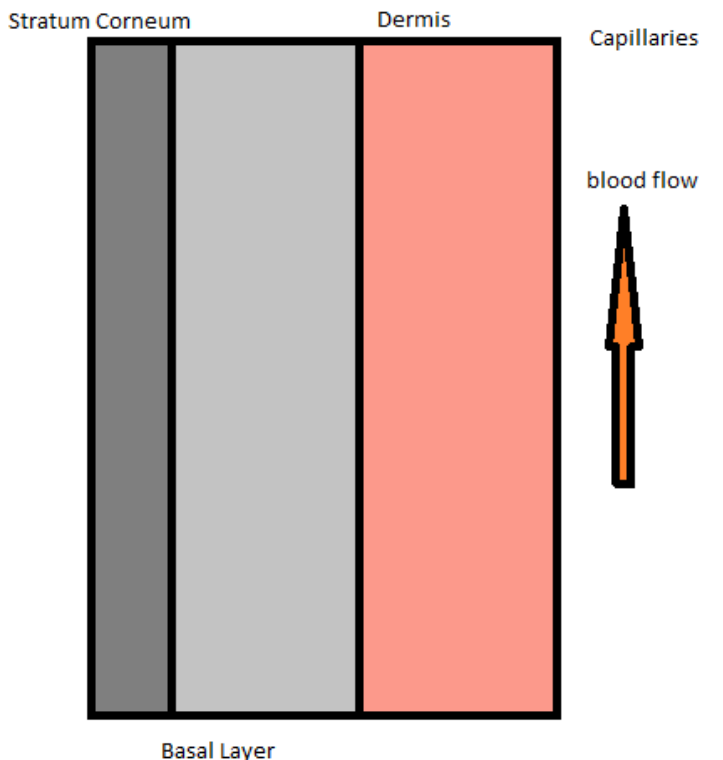


Figure 2: Representation of the skin model used in the problem solving. The patch application is at the outer edge of the stratum corneum (left side of figure), where flux is set to zero. The inside edge is the interface between the dermis and the capillaries. For the analytical solution, all three layers were assumed to have the same diffusion coefficient, and therefore effectively became one slab.

Analytical Solution

Partial Differential Equation – Fick's Law: $\frac{\partial c}{\partial t} = D \frac{\partial^2 c}{\partial x^2}$

Boundary Conditions: $\left. \frac{\partial c}{\partial x} \right|_{x=0} = 0 ; c(L, t) = 0$

Initial Conditions: $c(x, 0) = c_0 \delta(x)$

$$c(x, t) = \varphi(x) * G(t)$$

$$\varphi(x) \frac{\partial G}{\partial t} = DG(t) \frac{\partial^2 \varphi}{\partial x^2} \rightarrow \frac{1}{DG} \frac{dG}{dt} = \frac{1}{\varphi} \frac{d^2 \varphi}{dx^2} = -\lambda^2$$

$$\frac{1}{DG} dG = -\lambda^2 dt \rightarrow G(t) = G_0 e^{-\lambda^2 D t}$$

$$\frac{1}{\varphi} \frac{d^2 \varphi}{dx^2} = -\lambda^2 \rightarrow \varphi(x) = c_1 \cos \lambda x + c_2 \sin \lambda x$$

$$\left. \frac{\partial c}{\partial x} \right|_{x=0} = 0 \rightarrow (-\lambda c_1 \sin \lambda x + \lambda c_2 \cos \lambda x) G_0 e^{-\lambda^2 D t} = 0$$

$$-\lambda c_1 \sin \lambda * 0 + \lambda c_2 \cos \lambda * 0 = 0 \rightarrow c_2 = 0$$

$$c(L, t) = 0 \rightarrow c_1 \cos \lambda L G_0 e^{-\lambda^2 D t} = 0$$

$$c_1 \cos \lambda L = 0 \rightarrow \lambda L = \frac{(2n+1)\pi}{2} \rightarrow \lambda = \frac{(2n+1)\pi}{2L}$$

$$c(x, t) = \sum_{n=0}^{\infty} c_n \cos \frac{(2n+1)\pi x}{2L} e^{-D \left[\frac{(2n+1)\pi}{2L} \right]^2 t}$$

$$c_n = \frac{2}{L} \int_0^L c_0 \delta(x) \cos \frac{(2n+1)\pi x}{2L} dx$$

$$c_n = \frac{2}{L} c_0$$

Final Solution:

$$c(x, t) = \sum_{n=0}^{\infty} \frac{2}{L} c_0 \cos \frac{(2n+1)\pi x}{2L} e^{-D \left[\frac{(2n+1)\pi}{2L} \right]^2 t}$$

MATLAB Analytical Solutions

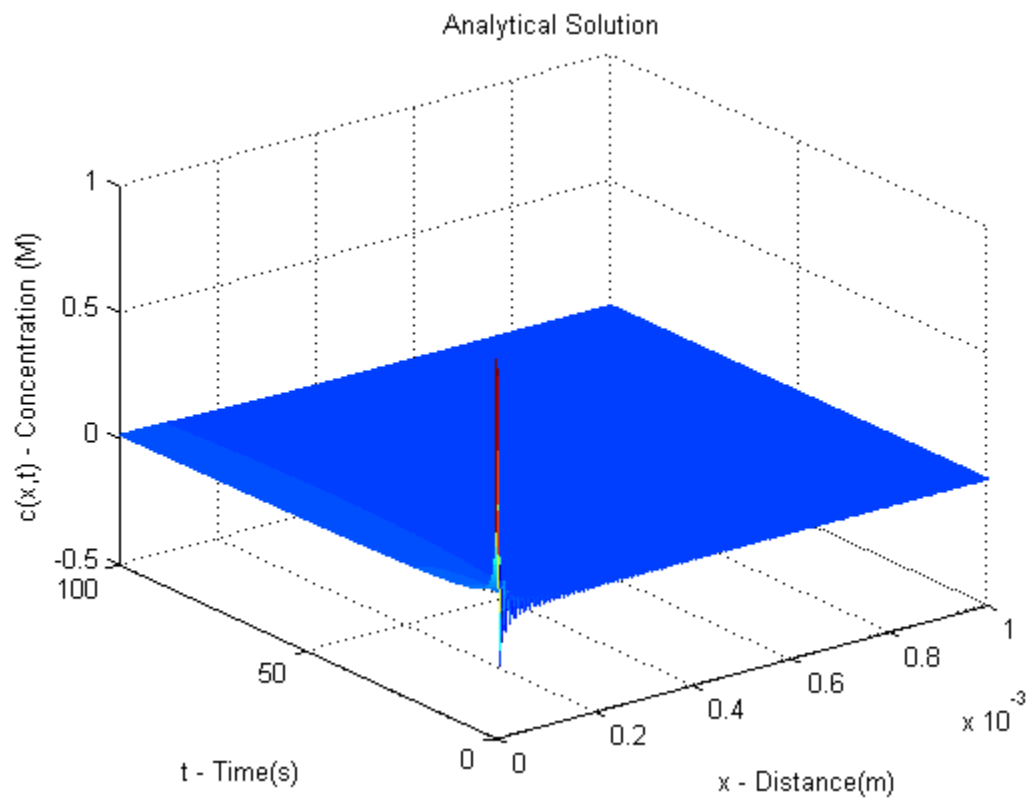


Figure 3: Surface plot of analytical solution approximated using the first 200 terms of the series.

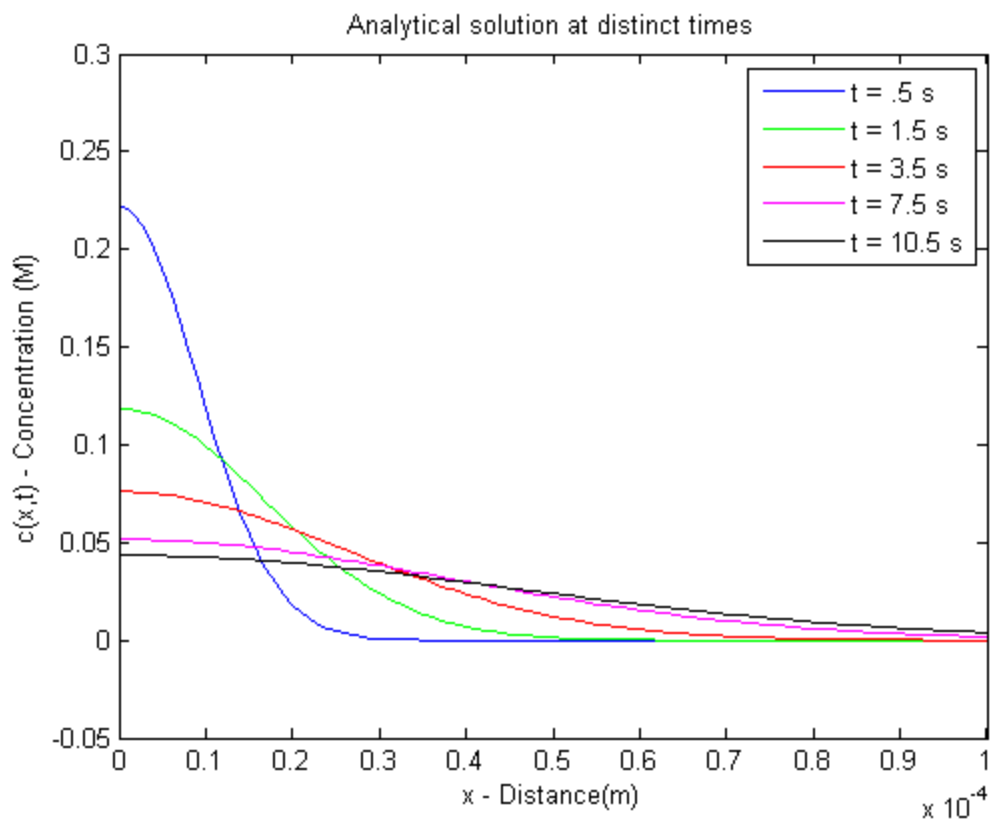


Figure 4: Variation of concentration over thickness of the skin of the analytical solution at distinct time points.

MATLAB Numerical Analysis

1-Slab Model

In the simplest model, the skin was modeled as one slab of thickness L with constant diffusivity D. This model makes the basic assumption that the skin is a homogenous slab of skin with constant thickness and diffusivity. It assumes that the impulse in concentration diffuses through only 1 compartment in the skin towards the sink at the location of the capillaries. This model can be applied to diffusion across the skin under the assumption that the stratum corneum serves as the only barrier to drug diffusion and that it spans the entire skin thickness. The boundary and initial conditions of this model were the same as the analytical model. The diffusivity of this slab, D₁, was estimated to be approximately 10^{-10} cm²/s. The thickness of the slab was approximated to be 1 mm. For the numerical analysis, the concentration at t = 0 and x = 0 was designated to be 1 molar.

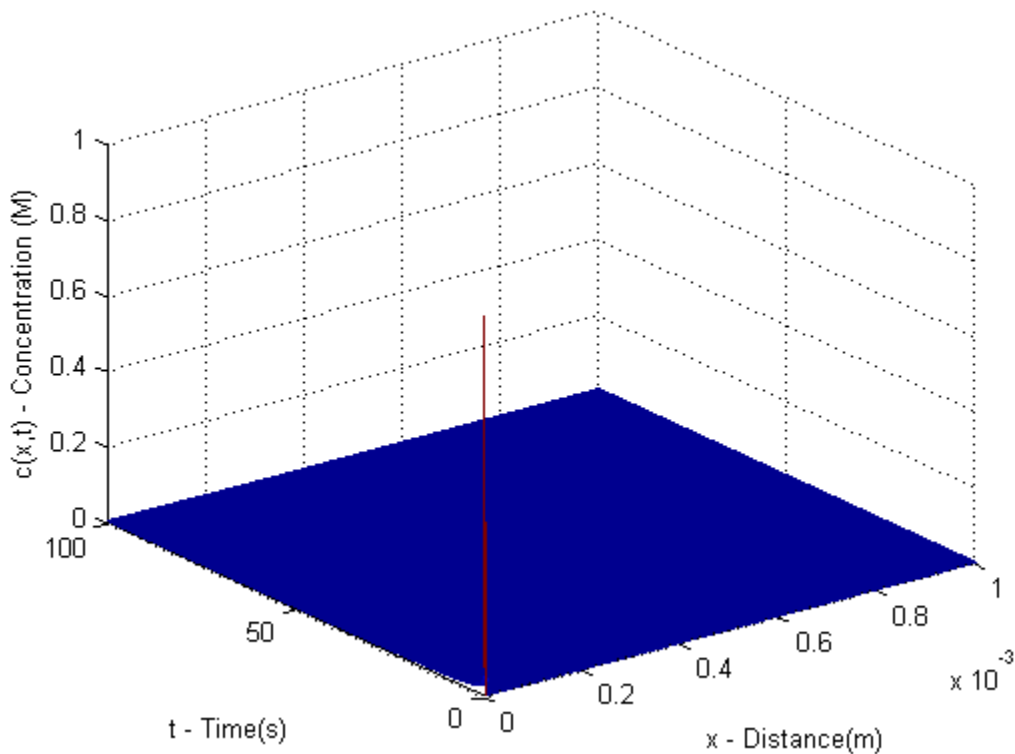


Figure 5: Surface plot of PDEPE numerical analysis of the 1-slab model

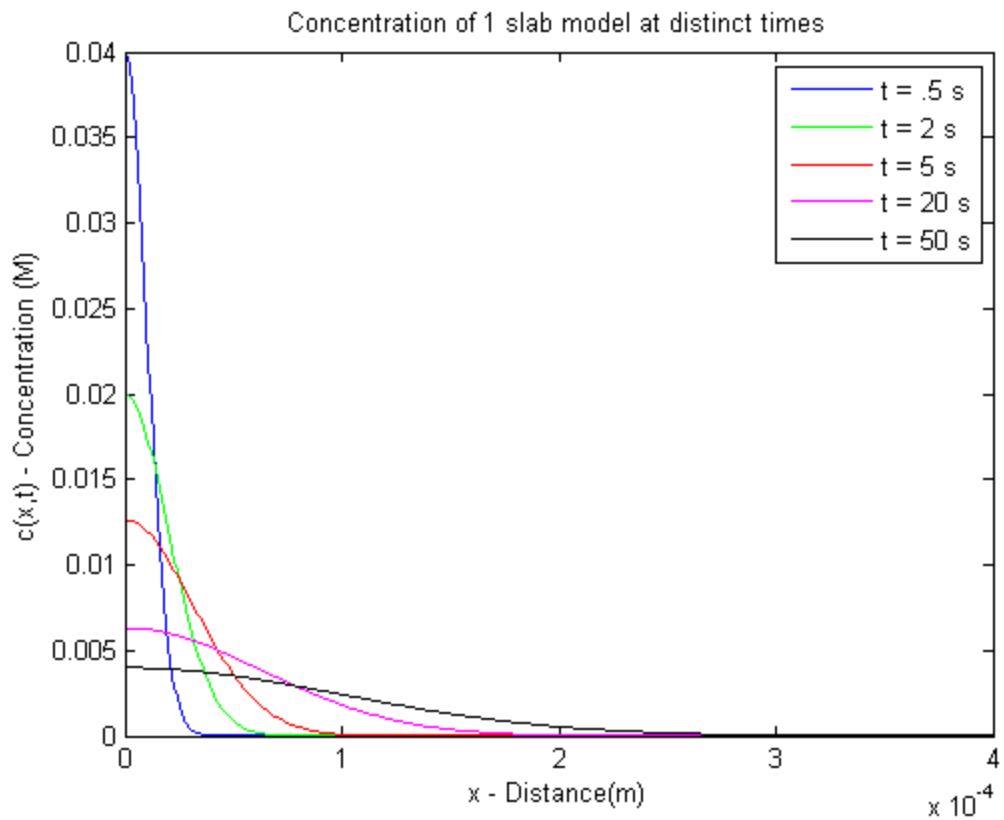


Figure 6: Variation of concentration over thickness of the skin of the MATLAB numerical analysis of the 1-slab model at distinct time points

2-Slab Model

This model served to provide a slightly more accurate representation of the heterogeneity of the layers in the skin. The stratum corneum and the epidermis of the skin were modeled to be 2 slabs in series, with different diffusion coefficients. This model takes into account the variation of diffusivity across the skin, where the hydrated layer, the epidermis, has a greater diffusion coefficient than the dry stratum corneum. The outer slab, modeling the stratum corneum, was estimated to be 1/40th of the entire thickness of the skin and was designated a diffusion coefficient, D1, of $10^{-10} \text{ cm}^2/\text{s}$. The inner slab, modeling the epidermis, was estimate to be 39/40^{ths} of the thickness of the skin with a higher diffusion coefficient, D2, of $10^{-6} \text{ cm}^2/\text{s}$. The total thickness of the two slabs was estimated to be 1 mm. For the numerical analysis, the initial concentration at $x=0$ and $t=0$ was designated to be 1 molar.

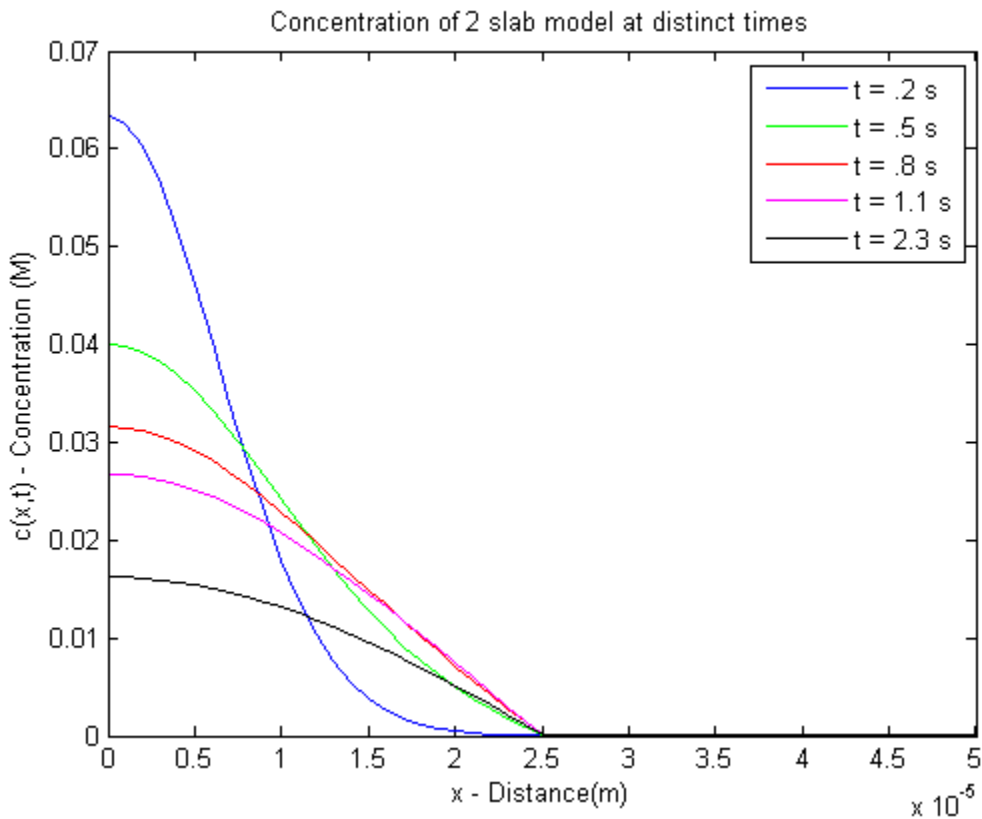


Figure 7: Variation of concentration over thickness of the skin of the MATLAB numerical analysis of the 2-slab model at distinct time points

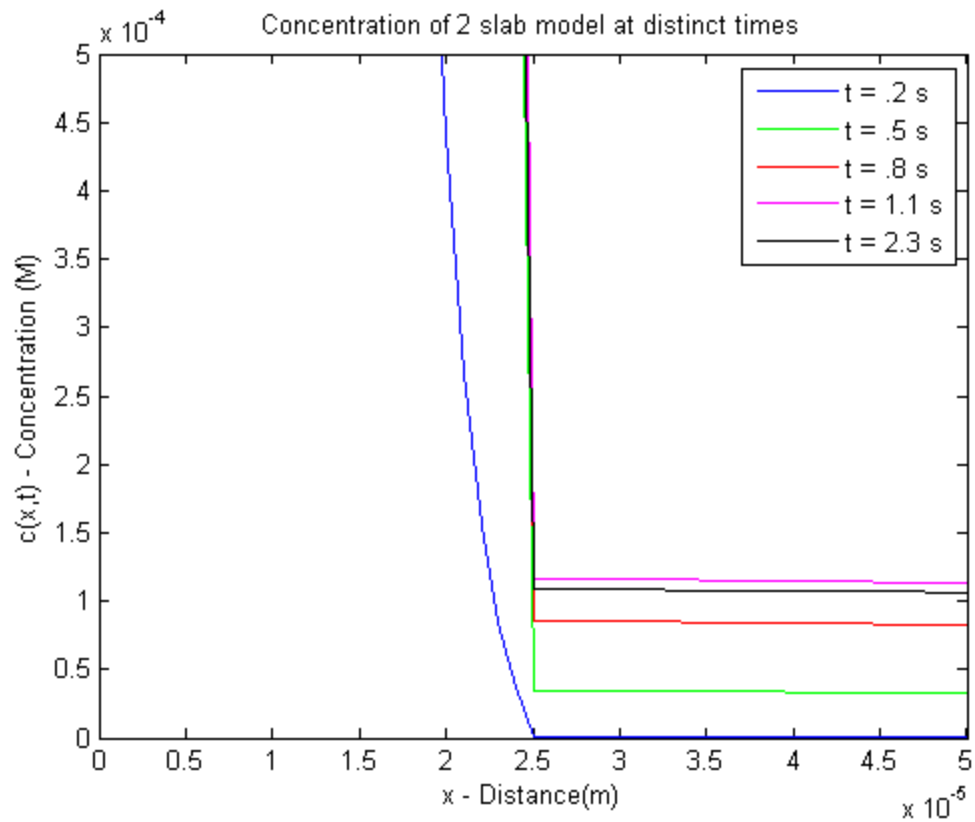


Figure 8: Variation of concentration across the interface in MATLAB numerical analysis of the 2-slab model at distinct time points

3-Slab Model

This model served to account for the slight differences in the properties of the epidermis and the dermis. The skin was modeled to be 3 slabs with the stratum corneum on the outside, the epidermis in the middle and the dermis located adjacent to the capillaries. The outer slab, modeling the stratum corneum, was estimated to be $1/32^{\text{nd}}$ of the entire thickness of the skin and was designated a diffusion coefficient, D1, of $10^{-10} \text{ cm}^2/\text{s}$. The center slab, modeling the epidermis, was estimate to be $15/32^{\text{nds}}$ of the thickness of the skin with a higher diffusion coefficient, D2, of $10^{-6} \text{ cm}^2/\text{s}$. The inner slab, modeling the dermis, was estimated to be $1/2$ the thickness of the skin with a diffusion coefficient, D3, of $10^{-5} \text{ cm}^2/\text{s}$. The total thickness was estimated to be 1 mm. For the numerical analysis, the initial concentration at $x=0$ and $t=0$ was designated to be 1 molar.

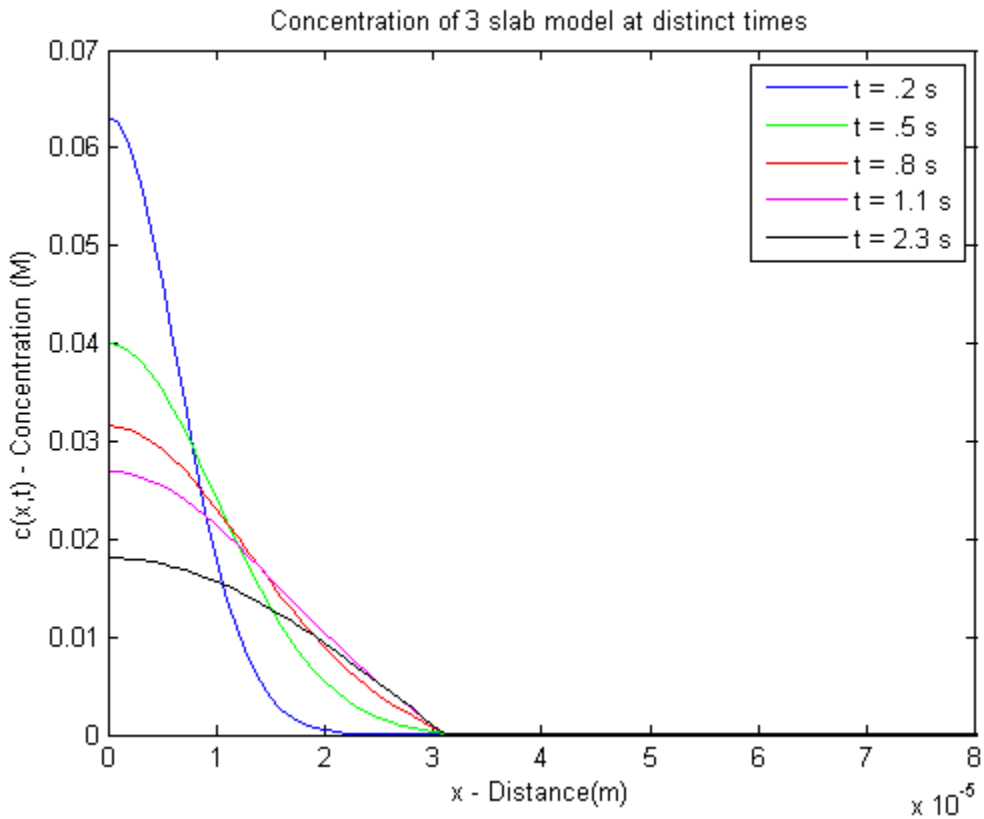


Figure 9: Variation of concentration over thickness of the skin of the MATLAB numerical analysis of the 3-slab model at distinct time points

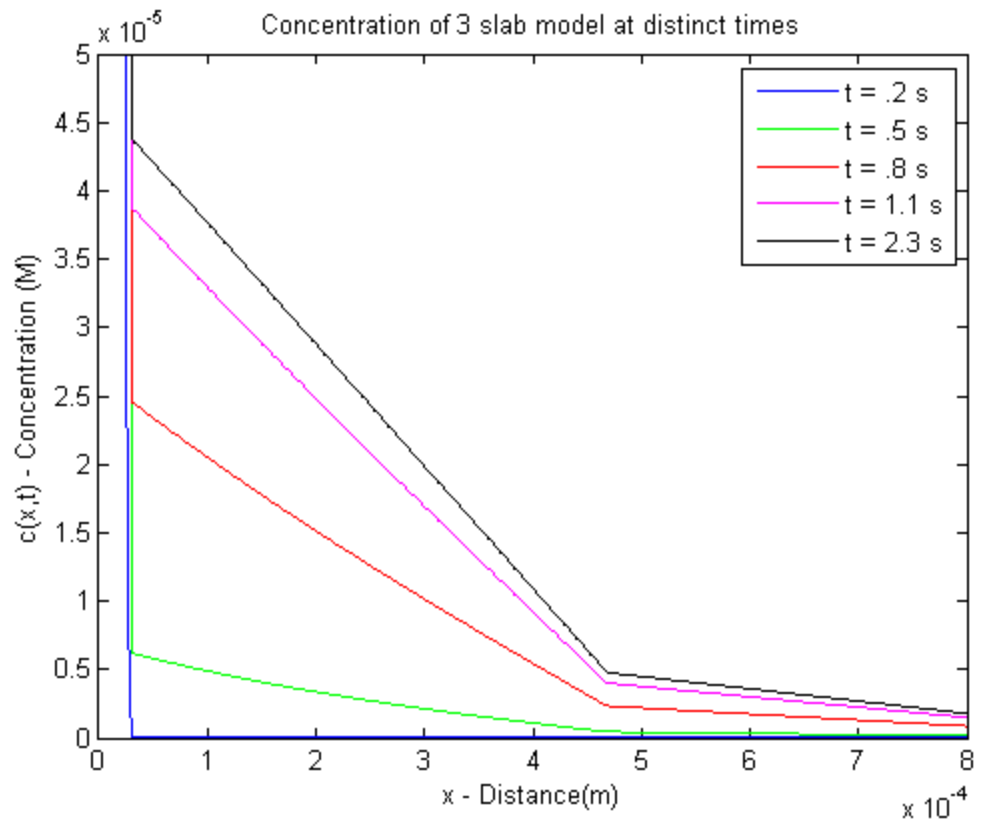


Figure 10: Variation of concentration across the interfaces in MATLAB numerical analysis of the 3-slab model at distinct time points

Linear Diffusivity Slab Model

In this model, the diffusivity of the skin was modeled to be dependent on the spatial position. This model was intended to represent a linear change in diffusivity from that of the stratum corneum to that of the capillary interface. The diffusion coefficient relation is given by the expression $D_1 + (D_2 - D_1) * x/L$. For the numerical analysis, the thickness was estimated to be 1 mm with an initial concentration designated to be 1 molar.

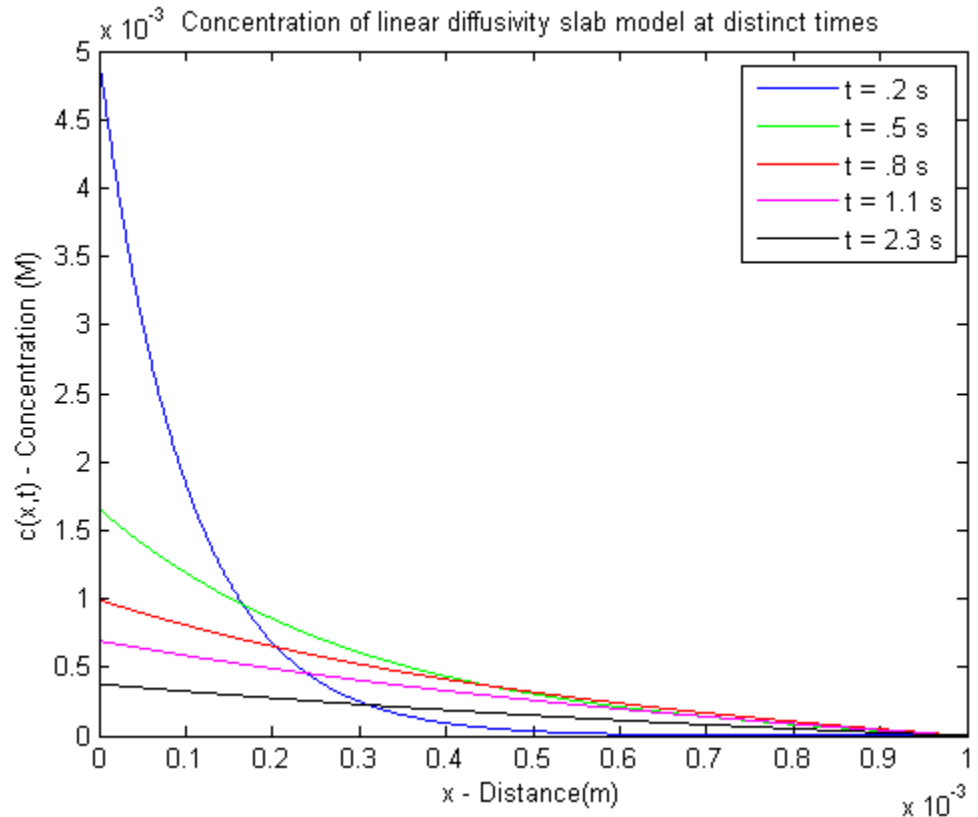


Figure 11: Variation of concentration over thickness of the skin of the MATLAB numerical analysis of the 2-slab linear diffusivity model at distinct time points

Hyperbolic Diffusivity Slab Model

In this model, the diffusion coefficient of the skin was modeled to be more representative of the spatial dependence. This model was intended to represent a hyperbolic change in diffusivity from that of the stratum corneum to that of the capillary interface. The diffusion coefficient relation is given by the expression $D_1 + (D_2 - D_1) * (1 - e^{-kx})$. For the numerical analysis, the thickness was estimated to be 1 mm with an initial concentration designated to be 1 molar. Furthermore, the constant k was chosen based upon the relation of diffusivity to thickness such that the diffusion coefficient was D_2 for 90% of the thickness of the skin.

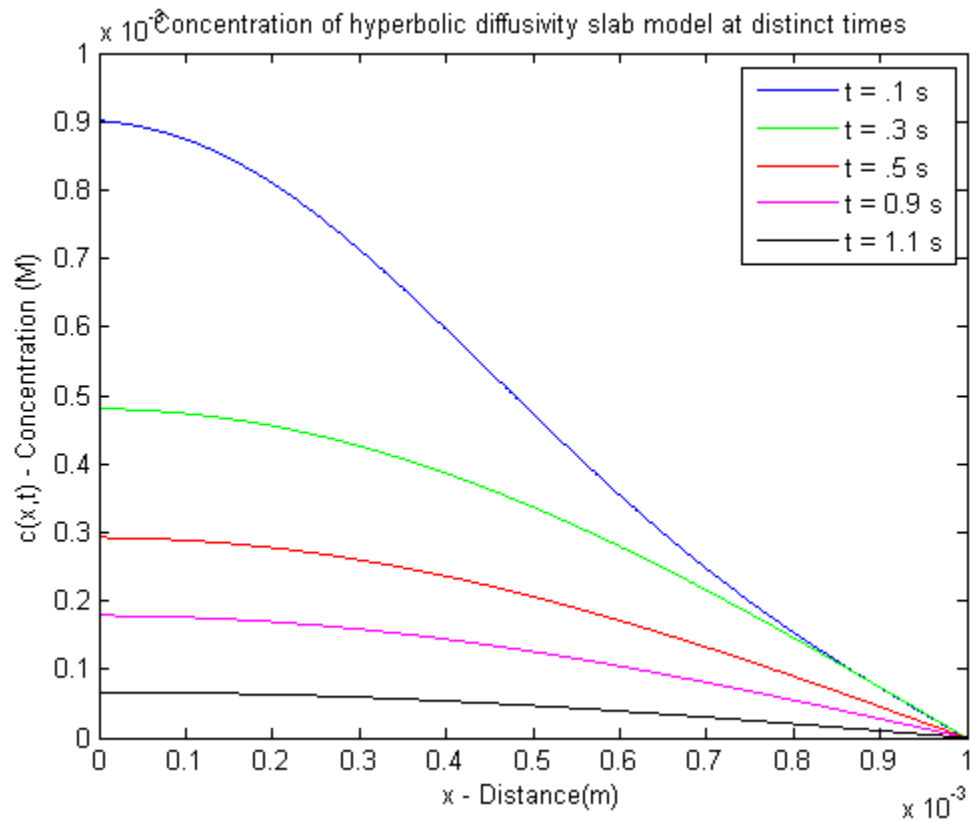


Figure 12: Variation of concentration over thickness of the skin of the MATLAB numerical analysis of the 2-slab hyperbolic diffusivity model at distinct time points

Discussion

Fick's Law was used to quantitatively model the simplified diffusion of particles across skin when an infinitely thin patch is placed on the outside of the stratum corneum. The homogeneous equation and boundary conditions that described the simplified model enabled solving the diffusion problem using separation of variables. The behavior of the analytical solution was according to expectations, as a half-Gaussian distribution decaying over time. This behavior is characteristic of the passive diffusion of a finite quantity that is bounded by zero flux at the source point and zero boundary condition at the limit of the spatial interval. The surface plot, Figure 3, demonstrated the exponential decay over space and time. The time section plots demonstrated the decay in the Gaussian distributions as the amplitude decreased over time and expanded in breadth.

The numerical analysis of the 1-slab model demonstrated similar behavior but it decayed faster than the analytical solution as seen in the surface plot, Figure 5. The immediate decay in time and space were more pronounced in this model in comparison to the analytical model which demonstrated oscillatory behavior in the initial time steps. This simple numerical analysis did show a similar decay in the Gaussian distribution over time and space as the amplitude decreased and the spread increased over time. This model decayed much more rapidly than the analytical model and achieves lower concentrations after shorter periods.

The 2-slab model demonstrated interesting behavior over time. As seen in Figures 7 and 8, there was a distinct decay in the model at the point in space corresponding to the interface of the two regions. The concentration decreased to nearly zero at this point in space. A plot of the concentration at this interface indicated the presence of extremely low concentrations that are negligible when compared to the initial behavior. This related to the biological phenomenon where stratum corneum limited diffusion much more than the other layers. An evolution of the initial Gaussian distribution is apparent as its behavior becomes distinctly parabolic at approximately $t = 0.8\text{--}1.1$ s time step. The decay of this model is on the same time scale as the 1-slab model.

The numerical analysis of the 3-slab model, depicted in Figures 9 and 10, demonstrated a similar behavior to the 2-slab model. The plot indicates that the concentration drops to very small values at the first interface in a similar manner to the previous model. Additionally, there is a transformation of the initial Gaussian distribution into a parabolic behavior at approximately $t = 1.1$ s time step. A closer look at the variation of the concentration across the two interfaces in this model, shown in Figure 10, reveals linear distribution of concentration across the other two slabs. The middle slab demonstrates a greater variation in concentration that can be appropriately attributed to its lower diffusivity compared to the last slab. Overall, the behavior of this model is on the same time scale as the 2-slab model, with the most significant distinction being the difference in location of the first interface.

The linear diffusivity slab model, plotted in Figure 11, was established to perform a numerical analysis of the diffusion across a slab where the diffusivity increased linearly with the spatial position. This model was intended to more accurately represent variations of diffusivity in skin due to inhomogeneous mixtures of cell types. This simplified model demonstrated an exponential decay that rapidly decreased with time and space. One should note that despite having the same time scale as the 2-slab and 3-slab models, this model displays concentrations approximately 10^{-3} times lower than the other two models.

The hyperbolic diffusivity slab model was a modification of the linear diffusivity slab model in order to represent the variation in more realistic fashion. The diffusivity expression was formulated to display steep increase in diffusivity over a small interval between the two regions, designated as the interface. Furthermore, this model does not assume that the stratum corneum has a constant diffusion, but it assumes that the diffusivity increases as the solute traverses this layer. This model shows a bell shaped distribution of concentration over the thickness of the skin. It displays a rapid decrease in concentration over time. This model displays concentrations approximately 10 times lower than the 2-slab and 3-slab models. Though this model decays quite rapidly, it is not to the extent of the linear diffusivity model.

Limitations

There were two main limitations in the analytical and numerical solutions of these models. For the analytical solution, the approximation of the infinite series to the first 200 terms neglects many of the higher eigenmodes of diffusion. It also establishes an infinite value for the initial concentration which is contrary to the reality of such a phenomenon where the initial concentration is finite. To account for this feature of the analytical solution, the solution was scaled down appropriately to establish the initial concentration at $x=0$ and $t=0$ to be 1 molar to provide adequate means for comparison with the numerical methods.

The main limitation with the numerical analyses was in the representation of the initial condition as an impulse function. In this study, the initial conditions were modeled as finite quantity C_i at point $x=0$ with zero for all other x points. This is realistic representation of the initial conditions but it fails to adequately represent the mathematical description of a delta function.

Our problem formulation of the diffusion across skin has limitations that can be addressed in future works. First, we only consider 1-dimensional diffusion across the skin, whereas a more accurate model would consider diffusion across the other 2 spatial dimensions with their respective diffusion coefficients. Second, the simplifying assumptions regarding the inhomogeneity of skin need to be addressed to create more accurate models for diffusion across the skin. The thickness of the skin and its individual layers will not be constant in a given area but will depend on the spatial positions. Furthermore, the diffusivity of the skin cannot be modeled accurately as a constant due to differences in the cellular structure of the skin and their contribution to the diffusivity. Considering the spatial dependence of diffusivity, the hyperbolic function appears to be more reasonable in comparison to the linear model. However, this model can only be verified with experimental data. Third, the model must consider the membrane partition coefficient as well as the clearance rate of the diffusing solute. The membrane partition coefficient relates the ratio of the concentrations at the air-skin interface and accurately determines the amount of substance initially diffusing into the skin. The clearance rate determines the quantity of solute diffused out of the skin into the capillaries. In our models, we did not consider these two aspects of the drug diffusion.

Future Work

Future work in modeling the diffusion of solute across skin can be made more accurate by including specific inhomogeneous diffusion properties of the skin tissue. In addition, the

patch can be modeled with a volume rather than one with infinitely thin thickness. This would represent the actual conditions for the diffusion of therapeutic molecules, such as lidocaine, from a finite volume through the skin-patch interface. Other physiological considerations include clearance rate and partition coefficients that divide the different layers. Partition coefficients mathematically would create discontinuities of the concentration function at the interfaces, and modeling and solving would increase in complexity. Nevertheless, the accurate representation would be useful in understanding skin permeability.

Additionally, the skin would be better represented when all three spatial dimensions are included, rather than the one dimension used in this problem solving. Diffusion of solutes through the skin would involve all three dimensions, and to understand those effects through rigorous modeling would be beneficial.

References

1. Scheuplein, RJ. "Permeability of the Skin." Comprehensive Physiology. 1 January 2011. 299–322. <<http://onlinelibrary.wiley.com/doi/10.1002/cphy.cp090119/full>>.
2. Galer, BS., Rowbotham, MC., Perander J., Friedman, E. "Topical Lidocaine Patch Relieves Postherpetic Neuralgia more Effectively than a Vehicle Topical Patch: Results of an Enriched Enrollment Study." Pain. Volume 80, Issue 3, 1 April 1999, Pages 533-538. <<http://www.sciencedirect.com/science/article/pii/S0304395998002449>>.
3. "Postherpetic Neuralgia." PubMed Health. A.D.A.M., Inc. 28 June 2011. <<http://www.ncbi.nlm.nih.gov/pubmedhealth/PMH0004666/>>.
4. "Shingles: Hope through Research." National Institute of Neurological Disorders and Stroke. 23 June 2011.
5. "Topical Lidocaine (a Local Anaesthetic) for the Treatment of Postherpetic Neuralgia (Nerve Pain)." PubMed Health. John Wiley & Sons, Ltd. 1 July 2008. <<http://www.ncbi.nlm.nih.gov/pubmedhealth/PMH0013059/>>.

Appendix – MATLAB Codes and Scan of Analytical Solution

MATLAB Codes for Numerical Simulations

```
global D1 D2 D3 Ci L
D1 = 10^-10; %cm^2/s

D2 = 10^-6;
D3 = 10^-5;
Ci = 1; % 1 micromolar
L = .001; %200 microns
```

Analytical Solution

```
for n = 0:200
    for i = 1:length(t)
        for j = 1:length(x)
            c1(i,j) = c1(i,j)+2/L*Ci*cos((2*n+1)*pi*x(j)/(2*L))*exp(-
D1*((2*n+1)*pi/(2*L))^2*t(i));
        end
    end
end
c1 = c1/c1(1,1); %scaling to account for infinite value at c1(0,0)

figure
mesh(x,t,c1)
% Az -12 El -6
xlabel('x - Distance(m)')
ylabel('t - Time(s)')
zlabel('c(x,t) - Concentration (M)')
title('Analytical Solution')

pAn1 = c1(5,:);
pAn2 = c1(15,:);
pAn3 = c1(35,:);
pAn4 = c1(75,:);
pAn5 = c1(105,:);

figure
plot(x,pAn1,'b',x,pAn2,'g',x,pAn3,'r',x,pAn4,'m',x,pAn5,'k')
xlabel('x - Distance(m)')
ylabel('c(x,t) - Concentration (M)')
xlim([0 0.0001])
title('Analytical solution at distinct times')
legend('t = .5 s','t = 1.5 s','t = 3.5 s','t = 7.5 s','t = 10.5 s')
```

Numerical Solution for a 1 – Slab Model

```
t = linspace(0,100,1000);
x = linspace(0,L,1000);
ps = pdepe(0,@pdefun2,@ic2,@bc2,x,t);
figure
mesh(x,t,ps)
% Az -10 El -10
```

```

xlabel('x - Distance(m)')
ylabel('t - Time(s)')
zlabel('c(x,t) - Concentration (M)')

ps1 = ps(6,:);
ps2 = ps(21,:);
ps3 = ps(51,:);
ps4 = ps(201,:);
ps5 = ps(501,:);

figure
plot(x,ps1,'b',x,ps2,'g',x,ps3,'r',x,ps4,'m',x,ps5,'k')
xlabel('x - Distance(m)')
ylabel('c(x,t) - Concentration (M)')
xlim([ 0 0.0004])
title('Concentration of 1 slab model at distinct times')
legend('t = .5 s','t = 2 s','t = 5 s','t = 20 s','t = 50 s')

```

Numerical Solution for a 2 – Slab Model

```

psA = pdepe(0,@pdefun4,@ic2,@bc2,x,t);
figure
mesh(x,t,psA)
% Az -10 El -10
xlabel('x - Distance(m)')
ylabel('t - Time(s)')
zlabel('c(x,t) - Concentration (M)')

psA1 = psA(3,:);
psA2 = psA(6,:);
psA3 = psA(9,:);
psA4 = psA(12,:);
psA5 = psA(24,:);

figure
plot(x,psA1,'b',x,psA2,'g',x,psA3,'r',x,psA4,'m',x,psA5,'k')
xlabel('x - Distance(m)')
ylabel('c(x,t) - Concentration (M)')
xlim([0 2*L/40])
title('Concentration of 2 slab model at distinct times')
legend('t = .2 s','t = .5 s','t = .8 s','t = 1.1 s','t = 2.3 s')

figure
plot(x,psA1,'b',x,psA2,'g',x,psA3,'r',x,psA4,'m',x,psA5,'k')
xlabel('x - Distance(m)')
ylabel('c(x,t) - Concentration (M)')
xlim([0 2*L/40])
ylim([0 0.0005])
title('Concentration of 2 slab model at distinct times')
legend('t = .2 s','t = .5 s','t = .8 s','t = 1.1 s','t = 2.3 s')

```

Numerical Solution for a 3 – Slab Model

```

psB = pdepe(0,@pdefun6,@ic2,@bc2,x,t);

```

```

figure
mesh(x,t,psB)
% Az -10 El -10
xlabel('x - Distance(m)')
ylabel('t - Time(s)')
zlabel('c(x,t) - Concentration (M)')

psB1 = psB(3,:);
psB2 = psB(6,:);
psB3 = psB(9,:);
psB4 = psB(12,:);
psB5 = psB(24,:);

figure
plot(x,psB1,'b',x,psB2,'g',x,psB3,'r',x,psB4,'m',x,psB5,'k')
xlabel('x - Distance(m)')
ylabel('c(x,t) - Concentration (M)')
xlim([0 0.00008])
title('Concentration of 3 slab model at distinct times')
legend('t = .2 s','t = .5 s','t = .8 s','t = 1.1 s','t = 2.3 s')

figure
plot(x,psB1,'b',x,psB2,'g',x,psB3,'r',x,psB4,'m',x,psB5,'k')
xlabel('x - Distance(m)')
ylabel('c(x,t) - Concentration (M)')
xlim([0 0.0008])
ylim([0 0.00005])
title('Concentration of 3 slab model at distinct times')
legend('t = .2 s','t = .5 s','t = .8 s','t = 1.1 s','t = 2.3 s')

```

Numerical Solution for a 1- Slab Model with hyperbolic dependence of diffusivity on x

```

psc = pdepe(0,@pdefun5,@ic2,@bc2,x,t);
figure
mesh(x,t,psc)
% Az -10 El -10
xlabel('x - Distance(m)')
ylabel('t - Time(s)')
zlabel('c(x,t) - Concentration (M)')

psc1 = psc(2,:);
psc2 = psc(4,:);
psc3 = psc(6,:);
psc4 = psc(8,:);
psc5 = psc(12,:);

figure
plot(x,psc1,'b',x,psc2,'g',x,psc3,'r',x,psc4,'m',x,psc5,'k')
xlabel('x - Distance(m)')
ylabel('c(x,t) - Concentration (M)')
title('Concentration of hyperbolic diffusivity slab model at distinct times')
legend('t = .1 s','t = .3 s','t = .5 s','t = 0.9 s','t = 1.1 s')

```

Numerical Solution for a 1- Slab Model with linear dependence of diffusivity on x

```

psD = pdepe(0,@pdefun3,@ic2,@bc2,x,t);
figure
mesh(x,t,psD)
% Az -10 El -10
xlabel('x - Distance (m)')
ylabel('t - Time (s)')
zlabel('c(x,t) - Concentration (M)')

psD1 = psD(2,:);
psD2 = psD(4,:);
psD3 = psD(6,:);
psD4 = psD(8,:);
psD5 = psD(12,:);

figure
plot(x,psD1,'b',x,psD2,'g',x,psD3,'r',x,psD4,'m',x,psD5,'k')
xlabel('x - Distance (m)')
ylabel('c(x,t) - Concentration (M)')
title('Concentration of linear diffusivity slab model at distinct times')
legend('t = .2 s','t = .5 s','t = .8 s','t = 1.1 s','t = 2.3 s')

%%%%%%%%%%%%%
% PEDPE Function Definitions

% boundary conditions
```

Defined such that the following equation is true at the left and right boundaries.

$$P(x, t, c) + Q(x, t)(f(x, t, c, \frac{\partial y}{\partial x})) = 0$$

```

function [pl,ql,pr,qr] = bc2(xl,ul,xr,ur,t)
pl = 0;
ql = 1;
pr = ur;
qr = 0;
```

```

% initial condition
Defined as the values of c(x,0) = c_0δ(x)
function u0 = ic2(x)
global Ci
u0 = Ci * (x==0);
```

```

% PDEPE Functions
Defined such that the following equation is true at the left and right boundaries.
```

$$C\left(x, t, c, \frac{\partial c}{\partial x}\right) * \frac{\partial c}{\partial t} = x^{-m} * \frac{D\left(x^{-m} * f\left(x, t, c, \frac{\partial c}{\partial x}\right)\right)}{\partial x} + S(x, t, c, \frac{\partial c}{\partial x})$$

```

% 1-Slab PDE Function
function [c,f,s] = pdefun2(x,t,u,DuDx)
```

```

global D1
c = 1;
f = (D1)*DuDx;
s = 0;

% 2-Slab PDE Function
function [c,f,s] = pdefun4(x,t,u,DuDx)
global D1 D2 L
c = 1;
f = (((D1+D2)/2)+((D1-D2)/2)*(x<L/40)+((D2-D1)/2)*(x>L/40))*DuDx;
s = 0;

% 3-Slab PDE Function
function [c,f,s] = pdefun6(x,t,u,DuDx)
global D1 D2 D3 L
c = 1;
f = (D3+(D2-D3)*(x<=15*L/32)+(D1-D2)*(x<=L/32))*DuDx;
s = 0;

% 1-Slab Hyperbolic Diffusivity PDE Function
function [c,f,s] = pdefun5(x,t,u,DuDx)
global D1 D2
k = 40000;
c = 1;
f = (D1+(D2-D1)*(1-exp(-k*x)))*DuDx;
s = 0;

% 1-Slab Linear Diffusivity PDE Function
function [c,f,s] = pdefun3(x,t,u,DuDx)
global D1 D2 L
c = 1;
f = (D1+(D2-D1)*x/L)*DuDx;
s = 0;
%%%%%%%%%%%%%

```